Research Square

Preprints are preliminary reports that have not undergone peer review.
They should not be considered conclusive, used to inform clinical practice,
or referenced by the media as validated information.

A 4-DOF piezoelectric stage based on distributed electrode-excitation of piezoelectric unimorphs

Rahul Shukla

rahulshukla@rrcat.gov.in

Raja Ramanna Centre for Advanced Technology

Harshal B. Wagh

Raja Ramanna Centre for Advanced Technology

sumit Sumit

Raja Ramanna Centre for Advanced Technology

Hari Shankar Kumar Jha

Raja Ramanna Centre for Advanced Technology

Varun P. Sharma

Raja Ramanna Centre for Advanced Technology

S. R. Kane

Raja Ramanna Centre for Advanced Technology

S. K. Rai

Raja Ramanna Centre for Advanced Technology

Research Article

Keywords: Piezoelectric unimorph, UV lithography, Multi-DOF piezoelectric stage, Photochemical machining

Posted Date: September 7th, 2026

DOI: https://doi.org/10.21203/rs.3.rs-10596849/v1

License: This work is licensed under a Creative Commons Attribution 4.0 International License.
Read Full License

Additional Declarations: No competing interests reported.

Abstract

We report the development of a novel 4-DOF monolithic piezoelectric stage using distributed electrode-excitation of piezoelectric unimorphs. The movements include *X*-tilt, *Y*-tilt, *Z*-translations and *Z*-rotation. The electrode pattern and size of piezoelectric plates are the important parameters while designing the stage. Finite element simulation is done to design and characterize the piezoelectric stage. The static displacement of the piezoelectric stage for *X*-tilt, *Y*-tilt and *Z*-translation of the piezoelectric stage are 47 μm, 48.8 μm, and 41.8 μm at 100 volts DC, respectively, whereas *Z*-rotation is nearly 29.5 μm at 100 volts. Fabrication of piezoelectric stage is done and electrode of piezoelectric plates have been made by UV lithography. Both simulation and experimental results are compared.

1. Introduction

Miniaturized stages with multiple degrees of freedom (DOFs) have attracted considerable attention due to their wide range of applications in optical endoscopy (Tang et al. 2009), image stabilization (Chiou et al. 2010), optical waveguide alignment, probe-based microscopy (Yong and Moheimani 2010), laser beam steering (Lemke et al. 2019), adaptive optics, data storage systems (Chen et al. 2002) and calibration of inertial sensors such as gyroscopes and accelerometers (Piratla et al. 2012; Tang et al. 2013). These applications demand compact devices capable of precise motion control, large displacement range, low power consumption, high reliability, and high dynamic performance (Yong et al. 2012). Various actuation mechanisms, including electrostatic, electromagnetic, and piezoelectric actuation, have been investigated to realize such systems (Rizzello et al. 2015; Shan et al. 2015; Price et al. 2015; AbuZaiter et al. 2016; Coskun et al. 2017; Zhu et al. 2021; Sharma et al. 2026a). Among them, piezoelectric actuation offers significant advantages, including high positioning resolution, fast response, low power consumption, compact size, and ease of integration into monolithic structures (Shukla et al. 2012; Liu et al. 2018; Chang et al. 2024; Pan et al. 2026).

Kobayashi *et al.* (Kobayashi et al. 2005) developed MEMS-based 1D optical micro-scanners actuated by piezoelectric cantilevers, achieving optical scanning angles up to 25° at resonance frequencies between 4.1 and 6.0 kHz. Zhu *et al.* (Zhu et al. 2011) reported a piezoelectrically actuated tip–tilt–piston micromirror utilizing PZT unimorph actuators capable of two-axis rotational and piston motions, producing rotational scan angles of approximately 5° and piston displacements of 32 μm. Aktakka *et al.* (Aktakka et al. 2013a) presented a six-degree-of-freedom vibratory stage based on distributed excitation electrodes and PZT/Si unimorph T-beams to achieve both translational and rotational motions. In another study, Aktakka et al. (Aktakka et al. 2013b) reported a 3-DOF piezoelectric micro vibratory stage based on bulk-PZT/Si L-shaped unimorph beam suspensions optimized via finite element analysis, achieving > 2.3° tilt and 42 μm displacement in static mode. Although, MEMS-based and microfabricated piezoelectric systems have demonstrated effective multi-degree-of-freedom (multi-DOF) actuation, their realization typically requires complex and multi-step fabrication processes including bulk-PZT integration, substrate thinning and fine-scale micropatterning. Such requirements substantially increase fabrication complexity and cost. Therefore, developing multi-DOF piezoelectric stages that combine

structural simplicity, ease of fabrication, compactness, and efficient actuation remains an important research challenge. Piezoelectric stack actuators have been extensively used in macro size precision stages (Kenton and Leang 2010; Yong and Moheimani 2010; Yong et al. 2012; Tang and Li 2015; Ghafarian et al. 2020); however, bending-mode piezoelectric actuators have gained increasing attention because of their lower cost, ease of fabrication, reduced residual stress, and favorable compliance characteristics.

Fleming *et al.* (Fleming and Yong 2017) demonstrated an *XY* nanopositioning stage machined from a single piezoelectric sheet, achieving a travel range of 8.6 μm with a first resonance frequency of 597 Hz. Moore *et al*. (Moore et al. 2018) subsequently proposed monolithic serial-kinematic nanopositioners in which the flexures, actuators and sensors were integrated into a single piezoelectric structure, achieving sensitivities greater than 18 nm/V and resonance frequencies around 250 Hz. In a later work, Moore *et al*. (Moore et al. 2021) further demonstrated an *XY* nanopositioning stage employing in-plane bending actuators capable of achieving approximately 10 μm travel range while maintaining a compact monolithic architecture suitable for atomic force microscopy. Omidbeike *et al*. (Omidbeike et al. 2019) extended the concept to a five-axis monolithic nanopositioning platform capable of translational and rotational motions, providing translational travel ranges up to 26 μm and rotational motions approaching 884 μrad. These studies demonstrate the effectiveness of bending mode multi-DOF nanopositioning systems; however, these designs are often involve complex structures or fabrication processes.

Zhang *et al*. (Zhang et al. 2021) proposed a two-axis piezoelectric tilting mirror based on bonded piezoelectric composite beams, demonstrating low capacitance, fast response, high positioning accuracy and effective laser beam steering capability. Furthermore, Lemke *et al*. (Lemke et al. 2019) developed piezo-actuated adaptive prisms employing bimorph bending beams for monoaxial and biaxial beam steering, achieving tilt angles up to ± 3.7° with continuously tuneable optical deflection. Similarly, Zhang *et al.* (Zhang et al. 2023) developed a compact 3-DOF piezoelectric micromanipulator using distributed ceramic plates and cross-beam bending, achieving ~ 99 μm motion range with 15.74 nm resolution and demonstrating precise non-contact microsphere manipulation. In addition to the above, Chen and Tian (Chen and Tian 2021) proposed a compact three-DOF flexible nanopositioner based on unimorph piezoelectric actuators and compliant flexures, offering a low-cost design with relatively large stroke and simplified construction. Conventional cantilever-type unimorph actuators generally provide only a single out-of-plane DOF, whereas more advanced configurations, such as L-shaped beam arrangements and distributed-electrode structures, can realize three or more DOFs (tilting about the *X*- and *Y*-axes and translation along the *Z*-axis) (Aktakka et al. 2013b) at the expense of increased design and small fabrication complexity.

In this work, a monolithic piezoelectric stage is designed, fabricated, and experimentally characterized. The proposed stage consists of a specially designed non-active compliant structure (NCS) fabricated from brass and eight PZT-5H piezoelectric plates bonded onto the structure with a unique distributed electrode configuration. The proposed architecture aims to provide multiple degrees of freedom while maintaining structural simplicity, compactness, and ease of fabrication. The paper is organized as

follows. At the outset, the conceptual design and finite element analysis of piezo stage is illustrated in detail. Next, the dimensions of piezoelectric stage, piezoelectric electrode size and junction length are determined by finite element simulation for uniform tilting and translation. Here, junction length is the region joining the central square brass plate of the stage and the piezoelectric unimorphs. Finite element simulation is done in COMSOL Multiphysics software. Furthermore, fabrication of 4-DOF piezo stage is discussed where NCS is made by end milling and electrode of the piezo plates are patterned by photochemical machining using UV lithography (Sharma et al. 2023, 2026b). The bonding of NCS with piezo plates is done at the designated places by silver epoxy to carry out the experiments. Finally, simulation and experimental results are compared.

2. Conceptual design and finite element analysis of piezoelectric stage

A new piezoelectric stage with a sigma (σ)-shaped beam actuated by four piezoelectric plates is proposed. As shown in Fig. 1, the piezoelectric stage incorporates two sigma-shaped beams with a total of eight piezoelectric plates. Each piezoelectric actuator uses a distributed-electrode configuration to enable *Z*-rotation along with *X*- and *Y*-tilt and *Z*-translation, thereby achieving 4-DOF motion. The junction length plays a crucial role in ensuring uniform motion across all 4-DOF of the piezoelectric stage and is determined through finite element analysis. The junction refers to the region where the free end of the sigma-shaped beam connects to the stage, as illustrated in Fig. 1 near Nodes 1 and 4. The dimensions of the NCS and the piezoelectric plates are optimized for uniform tilting, translation and ease of fabrication.

An electromechanically coupled finite element model of the piezoelectric stage is developed in COMSOL Multiphysics. The linear constitutive equations of piezoelectricity are employed to couple the *Solid Mechanics* and *Electrostatics* physics modules for simulating the piezoelectric effect. Quadratic hexahedral elements are used to discretize both the NCS and piezoelectric plates, and the Lagrange formulation is applied to define the shape functions of the elements. Mesh refinement test was done to finalize the element size in the finite element analysis.

3. Fabrication of piezoelectric stage and experimental setup

The fabrication of the piezoelectric stage was carried out in three main steps: i) fabrication of the NCS from a 300 μm thick brass wafer, ii) patterning of distributed electrodes on the piezoelectric plates using photochemical machining, and iii) bonding of the piezoelectric plates onto the NCS with conductive silver epoxy. These fabrication steps are summarized in Fig. 2. The NCS was fabricated by end-milling a low-roughness (≈ 200 nm RMS) flat brass wafer using a CNC machine. The end-milled brass wafer is shown in Fig. 3(a). The dimensions of the PZT-5H piezoelectric plates are 30 mm × 5 mm × 0.55 mm (L × W × H). The length of the piezoelectric plates matches the length of the piezoelectric stage (30 mm), and their width is equal to the width of the sigma-shaped beam of the NCS. Distributed electrode patterns on the piezoelectric plates are created by photochemical machining. For this process, a photomask was

prepared, and the piezoelectric plates were spin-coated with a positive photoresist (AZ P4620). After spin coating, the photoresist was baked at 110°C, followed by a 34-second UV flood exposure. The exposed plates were then developed in AZ400K developer solution and rinsed with DI water. After UV lithography, the Ag electrode regions were selectively etched using an HNO_3 and DI water (1:10 ratio) etchant for about 5 minutes. The resulting distributed-electrode patterned piezoelectric plate is shown in Fig. 3(b). Both the NCS and the piezoelectric plates were bonded using silver epoxy (8331-14G, MG Chemicals, Canada). Copper wires

were attached to the distributed electrodes with silver epoxy to establish electrical contacts. For support, the piezoelectric stage was mounted on an acrylic fixture, which was placed on an *X*-*Y*-*Z* stage for characterization. Two DC power supplies were used to actuate the piezoelectric stage, and displacements were measured using a confocal displacement measurement sensor (IFS 2405-3, Micro-Epsilon, Ortenburg, Germany). The sensor was calibrated before each measurement for different node locations of the piezoelectric stage.

4. Results and discussion

First, the effects of junction length and electrode size on the performance of the piezoelectric stage were investigated. Finite element analysis of the stage was done in COMSOL Multiphysics to compute nodal displacements for different junction lengths and electrode sizes. The variation of nodal displacement with junction length for two electrode sizes (14 mm × 2 mm and 12 mm × 2 mm) are shown in Fig. 4. It is clear from Fig. 4 that the 14 mm × 2 mm electrode size exhibits greater nonuniformity in stage motion compared to the 12 mm × 2 mm configuration. Furthermore, a junction length of 5.5 mm × 1 mm yields the minimum error in motion uniformity. At a junction length of 5.5 mm × 1 mm and an electrode size of 12 mm × 2 mm, the *X*-tilt, *Y*-tilt, and *Z*-translation of the piezoelectric stage are measured as 47 μm, 48.8 μm, and 41.8 μm, respectively, at 100 V DC. The *Z*-rotation is approximately 29.5 μm at 100

V. The static analysis results are shown in Fig. 5, where contour plots visualize the uniformity of surface displacement for the *X*-tilt, *Y*-tilt, *Z*-translation, and *Z*-rotation, respectively. The tilting and translation movements are highly uniform, with a maximum error of less than 1 μm across all nodal combinations (refer Fig. 5). The piezoelectric stage was fabricated using the process discussed in Section 3, following the verification of movement uniformity through finite element analysis. After fabrication, the nodal displacements for the *X*- and *Y*-tilts were measured at 100 V using a confocal sensor.

The simulation and experimental results are compared, as shown in Fig. 6. For the *X*-tilt, nodes N_1 and N_3 move together, as do nodes N_2 and N_4. While the simulation results for these pairs are nearly identical, a significant difference is observed between the experimental and simulated results for nodes N_2, N_3, and N_4. The experimental displacement of nodes N_3 and N_2 are quite close to the simulation results, whereas the experimental displacement of nodes N_1 and N_3 is nearly 22 μm less than the simulated results. Similarly, for the *Y*-tilt, nodes N_1 and N_2 move together, as do N_3 and N_4. Again, a deviation between the experimental and simulation results is observed. Here, the experimental displacements of nodes N_1 and

N_4 are close to the simulation results, while the experimental displacement of nodes N_2 and N_3 is nearly 33 μm less than the simulated results. This deviation in the results is mainly due to the following reasons; i) Variation in the dimensions and piezoelectric properties of piezo plates and variation in distributed electrode formed by photochemical machining. ii) The d_{33} coefficient of piezoelectric plates are varied from 575 pC/N to 650 pC/N whereas thickness is varied from 0.5 mm to 0.6 mm. The length and width of the piezoelectric plates are also non-uniform. iii) The overall flatness of the piezoelectric stage is sacrificed due to the inclusion of silver epoxy at 32 places for making electrical contacts from the distributed-electrodes. iv) The variation in the epoxy strength of piezoelectric unimorphs which are used to bond 8 piezoelectric plates over NCS is also responsible for the deviation in same node for *X*- and *Y*-tilt. The deviation between experimental and simulation results can be minimized by addressing the aforementioned issues associated with 4-DOF piezoelectric stage. The measurement of *Z*- rotation could not be done due to the unavailability of resources. In this paper, a novel 4-DOF sigma shaped piezoelectric unimorphs based piezoelectric stage is conceptualized. The performance of *X*-tilt, *Y*-tilt, *Z*-translation and *Z*-rotation is quite encouraging due to its relatively simple manufacturing technique. Unlike L shaped beam with T cross section of Aktakka *et al.* (Aktakka et al. 2013b, a) we have proposed a novel sigma shaped beam with rectangular cross section which has greatly reduced the difficulties associated with the manufacturing of piezoelectric stage. The disadvantage lies with the non-availability of *X*- and *Y*-translations. Although in the current design the performance of *X*- and *Y*-translations is not impressive but there lies a strong possibility of further optimization of sigma shaped piezoelectric unimorphs for 6-DOF piezoelectric stage.

5. Conclusion

A novel 4-DOF piezoelectric stage is conceptualized, simulated, fabricated and characterized. The 4 DOFs are *X*- and *Y*-tilt, *Z*-translation and *Z*-rotation. The monolithic piezoelectric stage with distributed electrode-excitation is fabricated and tested. Nearly 45 μm displacement is achieved at 100 volts DC for *X*- and *Y*-tilt and *Z*-translation. The *Z*-rotation is 29.5 μm at 100 volts DC. At few places the experimental results are not in good agreement with the simulations results. The reasons of discrepancies are mainly attributed to dimensional variation in piezoelectric plates, difference in piezoelectric properties from plate to plate and extensive use of epoxy and associated variation in strength and flatness.

Declarations

AcknowledgementThe authors gratefully acknowledge the Computer Division of RRCAT for providing access to COMSOL Multiphysics. The support of Workshop A in the fabrication of the fixtures and NCS structure is also sincerely acknowledged.

Author contributions RS: Conceptualization, Methodology, Software, Validation, Formal analysis, Investigation, Writing - Original Draft, Resources, Writing - Review & Editing, Visualization, Supervision; HBW: Methodology, Investigation, Formal analysis, Visualization; Sumit: Software, Formal analysis, Visualization, Data Curation, Validation, Writing -Original Draft; HSKJ: Visualization, Data Curation, Writing

- Review & Editing; VPS: Data Curation, Writing - Review & Editing; SRK:, Resources; SKR: Resources, Supervision

Funding Information The authors acknowledge the financial support from Department of Atomic Energy, Govt of India however there was no support for the publication charges.

Conflicts of interest/Competing interests The author(s) declared no potential conflicts of interest with respect to the research, authorship, and/or publication of this article.

Ethics declaration: Not applicable

References

1. AbuZaiter A, Hikmat OF, Nafea M, Ali MSM (2016) Design and fabrication of a novel XYθz monolithic micro-positioning stage driven by NiTi shape-memory-alloy actuators. Smart Mater Struct 25:105004. https://doi.org/10.1088/0964-1726/25/10/105004
2. Aktakka EE, Peterson RL, Najafi K (2013a) A 6-DOF piezoelectric micro vibratory stage based on multi-axis distributed-electrode excitation of PZT / SI unimorph T-beams. In: Transducers & Eurosensors XXVII: The 17th International Conference on Solid-State Sensors, Actuators and Microsystems, Barcelona, Spain. pp 1583–1586
3. Aktakka EE, Peterson RL, Najafi K (2013b) A 3-Dof Piezoelectric Micro Vibratory Stage Based on Bulk-Pzt / Silicon Crab-Leg Suspensions. In: 2013 IEEE 26th International Conference on Micro Electro Mechanical Systems (MEMS), Taipei, Taiwan. pp 576–579
4. Chang Q, Chen W, Zhang S, et al (2024) Review on Multiple-Degree-of-Freedom Cross-Scale Piezoelectric Actuation Technology. Adv Intell Syst 6:2300780. https://doi.org/10.1002/aisy.202300780
5. Chen N, Tian C (2021) Design, modeling and testing of a 3-DOF flexible piezoelectric thin sheet nanopositioner. Sensors Actuators, A Phys 323:112660. https://doi.org/10.1016/j.sna.2021.112660
6. Chen T-L, Oldham K, Li Y, Horowitz R (2002) Suspension Vibration Compensation Using a MEMS Microactuator in Hard Disk Drives. IFAC Proc Vol 35:705–710. https://doi.org/10.1016/s1474-6670(17)34022-3
7. Chiou JC, Hung CC, Lin CY, Lin YJ (2010) Design, fabrication, and actuation of micro-electro-mechanical system-based image stabilizer. Jpn J Appl Phys 49:014201. https://doi.org/10.1143/JJAP.49.014201
8. Coskun MY, Sancak C, Itik M, Alici G (2017) Hybrid force and position control of a conducting tri-layer electro-active polymer actuator. Trans Inst Meas Control 39:288–296. https://doi.org/10.1177/0142331216659537
9. Fleming AJ, Yong YK (2017) An ultrathin monolithic XY nanopositioning stage constructed from a single sheet of piezoelectric material. IEEE/ASME Trans Mechatronics 22:2611–2618. https://doi.org/10.1109/TMECH.2017.2755659

10. Ghafarian M, Shirinzadeh B, Al-Jodah A, et al (2020) FEA-based optimization of a complete structure of a monolithic z/tip/tilt micromanipulator. J Micro-Bio Robot 16:93–110. https://doi.org/10.1007/s12213-020-00133-4
11. Kenton BJ, Leang KK (2010) Design, characterization, and control of a monolithic three-axis high-bandwidth nanopositioning stage. In: 2010 American Control Conference, Baltimore, USA. pp 4950–4956
12. Kobayashi T, Tsaur J, Maeda R (2005) Fabrication of optical micro scanner driven by PZT actuators. Jpn J Appl Phys 44:7078–7082. https://doi.org/10.1143/JJAP.44.7078
13. Lemke F, Weber PM, Wallrabe U, Wapler MC (2019) Piezo-Actuated Adaptive Prisms for Optical Scanning. In: Martínez-García A, Bhattacharya I, Otani Y, Tutsch R (eds) Progress in Optomechatronic Technologies . Springer Proceedings in Physics. Springer, Singapore, pp 85–91
14. Liu Y, Deng J, Su Q (2018) Review on Multi-Degree-of-Freedom Piezoelectric Motion Stage. IEEE Access 6:59986–60004. https://doi.org/10.1109/ACCESS.2018.2875940
15. Moore SI, Omidbeike M, Fleming A, Yong YK (2018) A monolithic serial-kinematic nanopositioner with integrated sensors and actuators. In: 2018 IEEE/ASME International Conference on Advanced Intelligent Mechatronics (AIM), Auckland, New Zealand. pp 150–155
16. Moore SI, Yong YK, Omidbeike M, Fleming AJ (2021) Serial-kinematic monolithic nanopositioner with in-plane bender actuators. Mechatronics 75:102541. https://doi.org/10.1016/j.mechatronics.2021.102541
17. Omidbeike M, Yong YK, Moore SI, Fleming AJ (2019) A five-axis monolithic nanopositioning stage constructed from a bimorph piezoelectric sheet. In: 2019 International Conference on Manipulation, Automation and Robotics at Small Scales (MARSS), Helsinki, Finland. pp 1–6
18. Pan Z, Wang L, Feng H, Jin J (2026) Multi-degree-of-freedom piezoelectric actuators: Recent advances and challenges. Int J Mech Sci 311:111197 Contents. https://doi.org/10.1016/j.ijmecsci.2026.111197
19. Piratla S, Lal A, Pandey M (2012) Nanogap ultrasonic actuator for non-contact control of levitated inertial sensor rotor. In: 2012 Solid-State, Actuators, and Microsystems Workshop Technical Digest. Transducer Research Foundation, San Diego, pp 82–85
20. Price AD, Naguib HE, Amara F Ben (2015) Electroactive polymer actuators for active optical components. J Intell Mater Syst Struct 26:2556–2564. https://doi.org/10.1177/1045389X14557505
21. Rizzello G, Naso D, York A, Seelecke S (2015) Modeling, identification, and control of a dielectric electro-Active polymer positioning system. IEEE Trans Control Syst Technol 23:632–643. https://doi.org/10.1109/TCST.2014.2338356
22. Shan G, Li Y, Zhang L, et al (2015) Contributed Review: Application of voice coil motors in high-precision positioning stages with large travel ranges. Rev Sci Instrum 86:101501. https://doi.org/10.1063/1.4932580
23. Sharma VP, Rai SK, Singh S, Shukla R (2026a) Probing the challenges in bulk micromachining of vertical comb-drive microactuators designed for manipulation of synchrotron radiation. Sensors

Actuators A Phys 404:117750. https://doi.org/10.1016/j.sna.2026.117750

24. Sharma VP, Rai SK, Singh S, Shukla R (2026b) Probing the challenges in bulk micromachining of vertical comb-drive microactuators designed for manipulation of synchrotron radiation. Sensors Actuators A Phys 404:117750. https://doi.org/10.1016/j.sna.2026.117750
25. Sharma VP, Shukla R, Mukherjee C, et al (2023) Study of metal-assisted chemical etching of silicon as an alternative to dry etching for the development of vertical comb-drives. J Micromanufacturing 6:19–26. https://doi.org/10.1177/25165984211033422
26. Shukla R, Lim LC, Gandhi P (2012) X-pod: a small footprint multi-legged piezoelectric single-crystal unimorph-based actuator concept. Smart Mater Struct 21:065015
27. Tang H, Li Y (2015) A new flexure-based Yθ nanomanipulator with nanometer-scale resolution and millimeter-scale workspace. IEEE/ASME Trans Mechatronics 20:1320–1330. https://doi.org/10.1109/TMECH.2014.2342752
28. Tang J, Green SR, Gianchandani YB (2013) Miniature wireless magnetoelastic resonant motor with frequency selectable bidirectional rotation. J Microelectromechanical Syst 22:730–738. https://doi.org/10.1109/JMEMS.2013.2242253
29. Tang S, Jung W, McCormick D, et al (2009) Design and implementation of fiber-based multiphoton endoscopy with microelectromechanical systems scanning. J Biomed Opt 14:034005. https://doi.org/10.1117/1.3127203
30. Yong YK, Moheimani SOR (2010) A compact XYZ scanner for fast atomic force microscopy in constant force contact mode. In: IEEE/ASME International Conference on Advanced Intelligent Mechatronics, Montréal, Canada. pp 225–230
31. Yong YK, Moheimani SOR, Kenton BJ, Leang KK (2012) Invited review article: High-speed flexure-guided nanopositioning: Mechanical design and control issues. Rev. Sci. Instrum. 83:121101
32. Zhang S, Liu Y, Deng J, et al (2021) Development of a low capacitance two-axis piezoelectric tilting mirror used for optical assisted micromanipulation. Mech Syst Signal Process 154:107602. https://doi.org/10.1016/j.ymssp.2020.107602
33. Zhang S, Zhao H, Ma X, et al (2023) A 3-DOF Piezoelectric Micromanipulator Based on Symmetric and Antisymmetric Bending of a Cross-Shaped Beam. IEEE Trans Ind Electron 70:8264–8275. https://doi.org/10.1109/TIE.2022.3213906
34. Zhu Y, Liu W, Jia K, et al (2011) A piezoelectric unimorph actuator based tip-tilt-piston micromirror with high fill factor and small tilt and lateral shift. Sensors Actuators, A Phys 167:495–501. https://doi.org/10.1016/j.sna.2011.03.018
35. Zhu Z, Chen L, To S (2021) A novel direct drive electromagnetic XY nanopositioning stage. CIRP Ann - Manuf Technol 70:415–418. https://doi.org/10.1016/j.cirp.2021.04.064

Figures

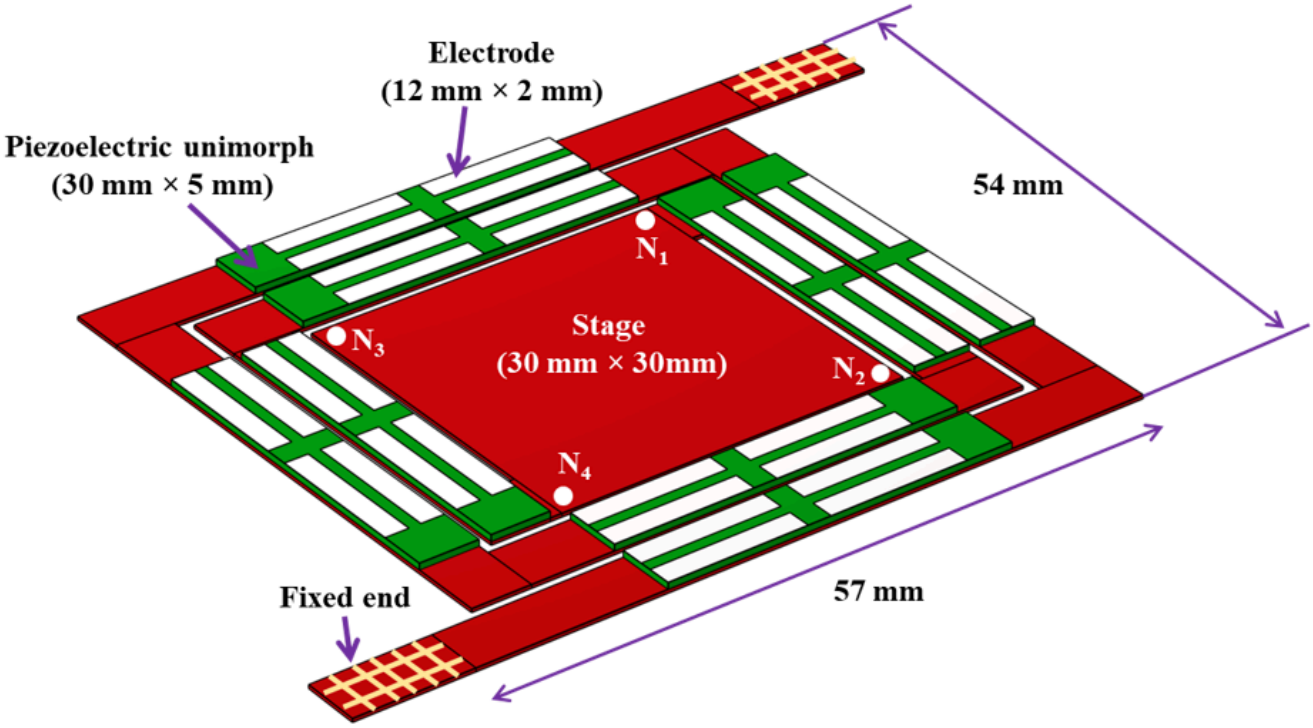


Figure 1

An isometric image of 4-DOF sigma (σ) shaped piezoelectric stage.

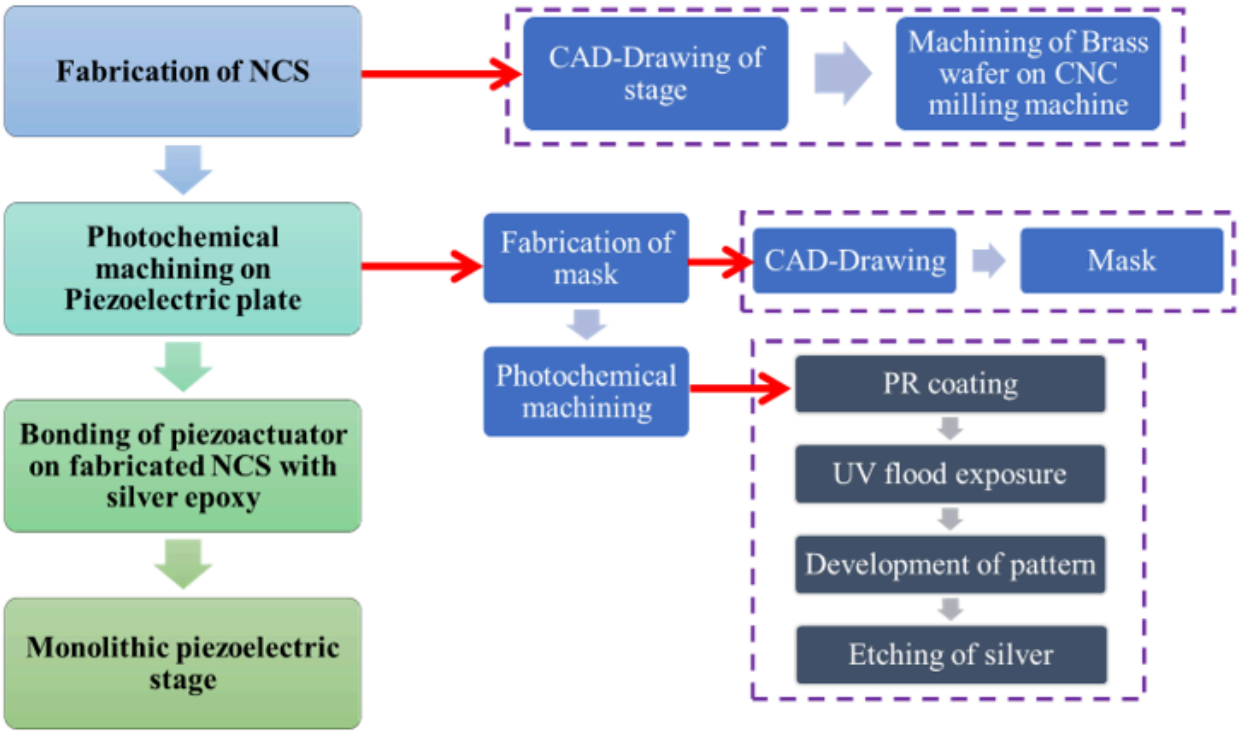


Figure 2

Flowchart showing the fabrication processes associated with NCS and piezoelectric plates of piezoelectric stage.

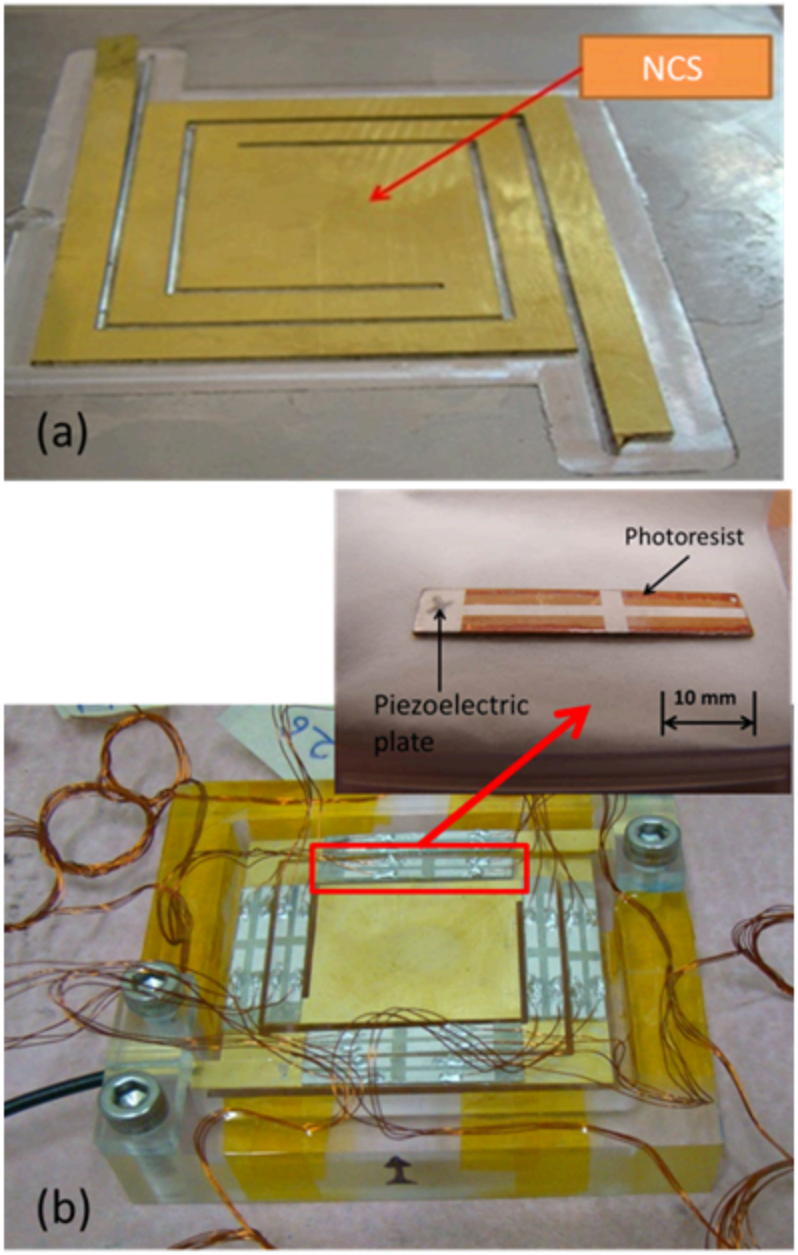


Figure 3

(a) An end-milled NCS from 300 μm thick good quality brass wafer, (b) piezoelectric stage carries an inset image of piezoelectric plate made by photochemical machining.

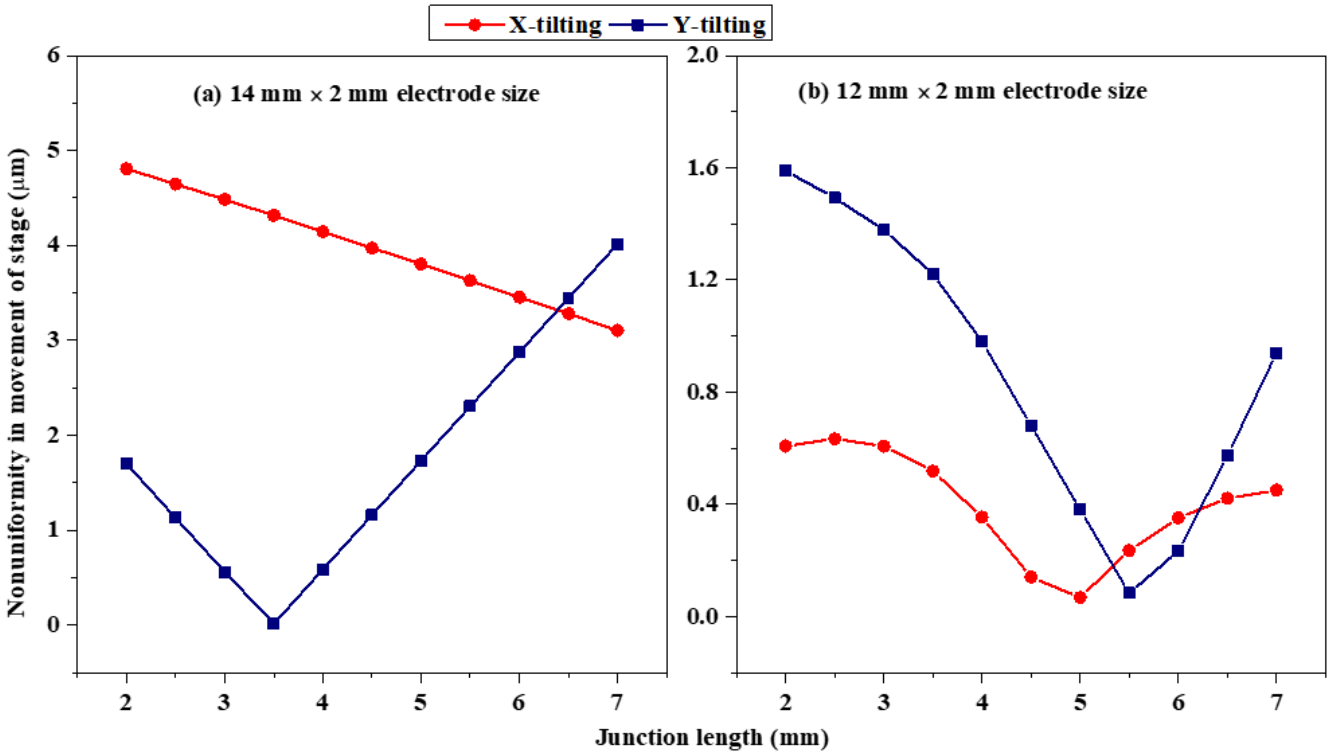


Figure 4

Nonuniformity in nodal displacement with respect to junction length at two electrode size (14 mm × 2 mm and 12 mm × 2 mm).

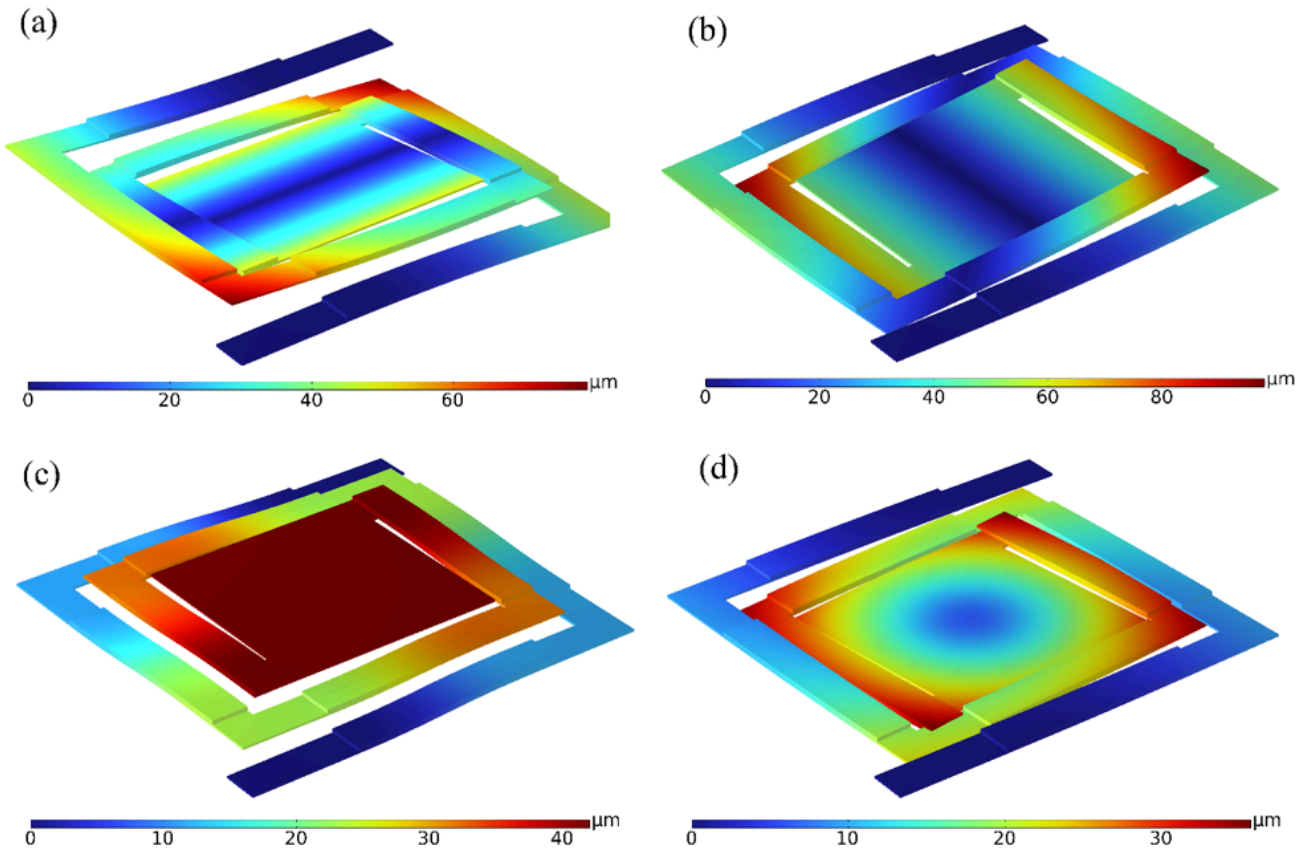


Figure 5

Contour plots showing the surface displacement of the 4-DOF piezoelectric stage when distributed electrode are excited at 100 volts DC: (a) *X*-tilt, (b) *Y*-tilt, (c) *Z*-translation and (d) *Z*-rotation.

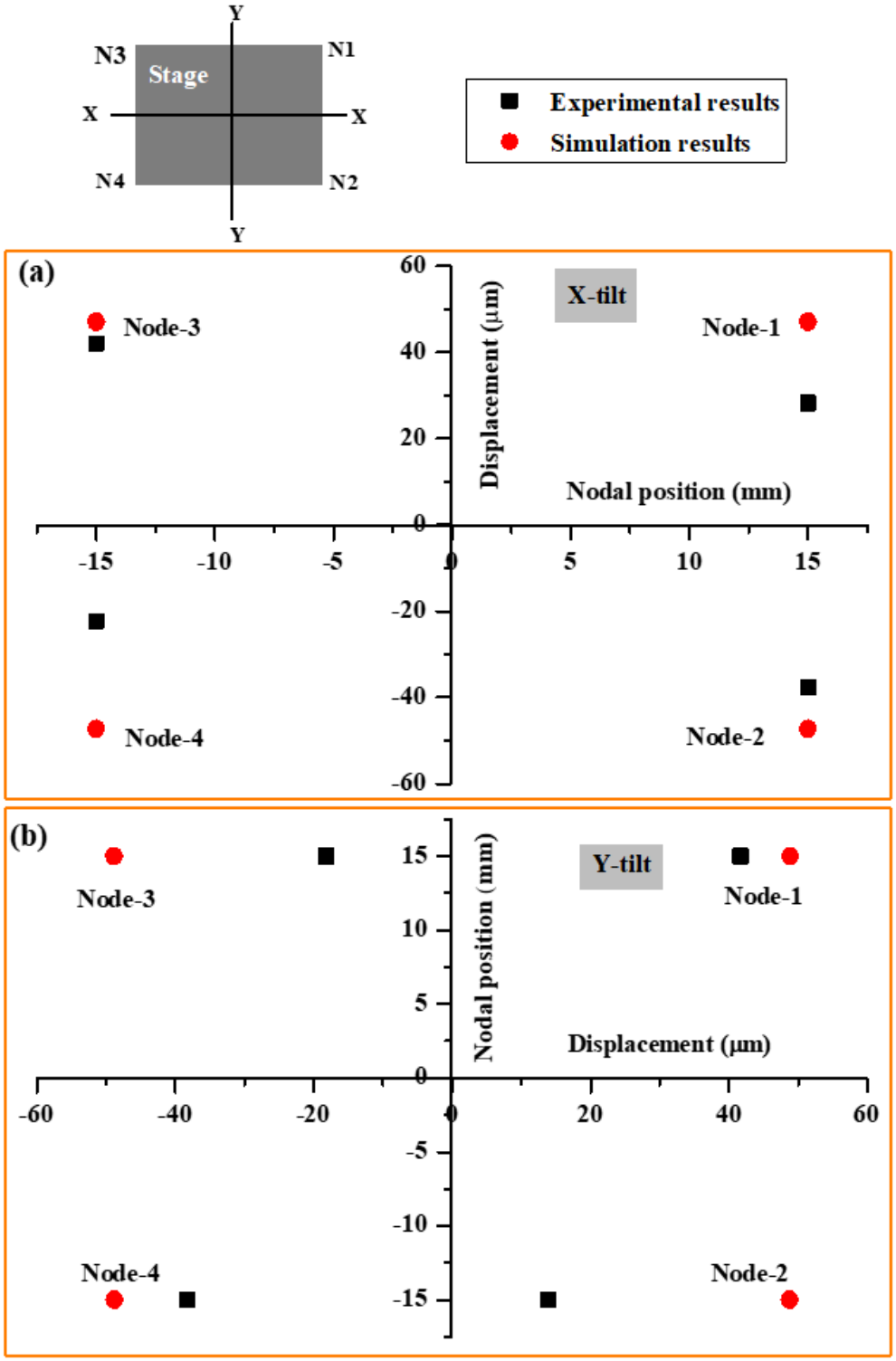


Figure 6

Comparison of experimental and simulation results for; (a) *X*-tilt and (b) *Y*-tilt. The comparison for all nodes is made